

NATIONAL AERONAUTICS AND SPACE ADMINISTRATION

PROPOSED ARTICLE FOR SYMPOSIUM PROCEEDINGS

CONTACT-SURFACE TAILORING IN REAL SHOCK TUBES

FACILITY FORM 602	N66 29459	
	(ACCESSION NUMBER)	(THRU)
	15	1
	(PAGES)	(CODE)
	TMX-56735	12
	(NASA CR OR TMX OR AD NUMBER)	(CATEGORY)

by Theodore A. Brabbs and Frank E. Belles

Lewis Research Center
Cleveland, Ohio

GPO PRICE \$

CFSTI PRICE(S) \$

Hard copy (HC) 1.00

Microfiche (MF) .50

4000 July 65

Prepared for

Proceedings of Fifth Shock Tube Symposium

July 30, 1965

65-55

FACILITY FORM 602

X65 37686 (ACCESSION NUMBER)	(THRU)
15 (PAGES)	2A (CODE)
(NASA CR OR TMX OR AD NUMBER)	12 (CATEGORY)

CONTACT-SURFACE TAILORING IN REAL SHOCK TUBES

by Theodore A. Brabbs and Frank E. Belles
Lewis Research Center
National Aeronautics and Space Administration
Cleveland, Ohio

ABSTRACT

The equilibrium pressure after interaction of a reflected shock with the contact surface can be confused with the tailored state, unless quantitative pressure measurements are made. Such measurements were used to find the true tailored conditions for $\text{CO}_2 + \text{Ar}$ and $\text{CO}_2 + \text{Ar} + \text{He}$ mixtures, and for N_2 driven by He. Calculated conditions in excellent agreement with these resulted when the real performance of the tube, instead of the ideal performance, was employed in the usual tailoring formula. This suggests a rapid systematic way to produce the tailored state, and shows that it will not be the same in all tubes. However, a small pressure excursion due to contact-surface interaction still remains even when perfect tailoring is achieved.

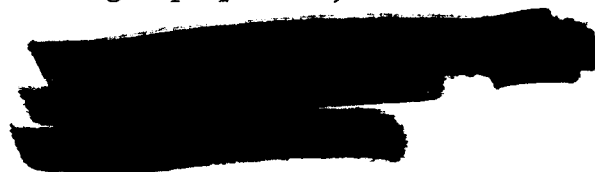
29459 ~~37686~~

Author

INTRODUCTION

In recent years considerable use has been made of the reflected shock wave in studying high temperature gas dynamic phenomena. Because it provides stationary test gas, increased testing time, higher gas enthalpy and density, and lends itself to chemical sampling, the reflected-shock technique has found wide usage in chemical shock tubes and shock tunnels. However, both applications require a detailed understanding and close control of the state of the gas behind the reflected shock wave. Because interaction between the reflected shock wave and the contact surface causes a pressure and temperature disturbance to be reflected back into the test zone, it is desirable to eliminate this interaction. This is usually accomplished by using the tailored-interface mode of operation.

In the tailored-interface mode, initial conditions in the driver (diaphragm pressure ratio, gas composition, and in some tubes, temperature) are adjusted so that the reflected shock wave, on encountering the contact surface, produces the same pressure and the same particle velocity on both sides of it. These requirements, when expressed in terms of the usual relations among shock strength and gas properties, lead to the tailoring formula



$$\frac{\alpha_4 + P_{25}}{\alpha_2 + P_{25}} = \frac{m_2(\gamma_2 - 1)T_{34}}{m_4(\gamma_4 - 1)T_{21}} \quad (1)$$

However, when this equation is used the calculations are usually made by assuming the shock tube behaves ideally; that is, the Mach number is related to the initial pressure ratio P_{41} by the ideal shock tube performance equations. Because most shock tubes do not behave ideally, the initial test conditions calculated from equation (1) are only approximate, and achievement of tailoring can be established only by observing the experimental pressure record. The experimental procedure usually employed is to calculate the initial tailoring conditions and to use these test conditions to obtain an experimental pressure record. If tailoring has not been achieved, which is the usual case, the initial pressure ratio (P_{41}) is adjusted somewhat and another pressure record is obtained. Because it is difficult to judge how much the pressure ratio must be changed by looking at the pressure record, the procedure usually requires several test runs. This procedure can be very time consuming and a simpler and more direct method for tailoring is desirable.

Ideally the tailored oscillogram is expected to show the reflected-shock pressure as a flat-topped plateau, and in principle there should be only one incident-shock Mach number that would yield such a record for a given driver-driven gas combination. In practice, however, records having the qualitative appearance described are obtained over a small range of incident Mach numbers close to the tailoring conditions. This is because the interaction is weak and has little effect on the pressure history. If, however, the shock tube is operated outside this range, the reflected shock wave will experience multiple reflections between the contact surface interface and the end of the tube. The result of these multiple shock reflections is the formation of a quasi-uniform region known as the "equilibrium" state (ref. 1). This equilibrium state like the tailored state is characterized by a flat-topped pressure history as shown in figure 1.

Figure 1 shows a typical nontailored pressure-time history. The arrival of the reflected disturbance from the contact surface can be seen by the abrupt change in the pressure. The flat region after the interaction is the equilibrium state. Thus a flat-topped pressure record is not always sufficient proof that tailoring has been achieved. Experimental results to be presented later show that confusion can exist between these two states and that a better criterion for tailoring is required.

At Mach numbers greater than the tailored one, the equilibrium pressure (p_e) is greater than the reflected shock pressure (p_5). Below the tailored Mach number, $p_e < p_5$. When tailoring has been achieved there is no interaction and $p_e = p_5$. Therefore, the criterion for tailoring chosen for this work was that the pressure after interaction be equal to the initial reflected shock pressure; that is, $P_{e5} = 1$. A plot of P_{e5} against M_s will yield the experimental tailored Mach number which can be compared with the calculated one.

The aims of the present work then were (1) to determine the tailored Mach number for several driver-driven gas combinations from the criterion $P_{e5} = 1$ and to compare it with the value calculated by means of equation (1), and (2) to develop a straightforward and rapid means of arriving at the tailored conditions without resorting to trial-and-error methods.

SYMBOLS

A_{ij} a_i/a_j

a sound speed

M_s incident shock Mach number

m molecular weight

P_{ij} p_i/p_j

p pressure

T temperature

T_{ij} T_i/T_j

U_{ij} u_i/a_j

u particle velocity

α $\frac{\gamma + 1}{\gamma - 1}$

β $\frac{\gamma - 1}{2\gamma}$

γ C_p/C_v ratio of specific heats

Subscripts:

e equilibrium region after interaction

1 undisturbed test gas

2 region behind incident shock wave

3 region behind contact surface

4 undisturbed driver gas

5 region behind reflected shock wave

APPARATUS

The shock tube was of the single-pulse type and was similar to that described by Glick, Squire, and Hertzberg (ref. 2). It was made up of sections of 6.35-centimeter inside-diameter stainless-steel tubing; the driven section was 3.2 meters long and the driver 1.88 meters. The dump tank volume was about 5600 liters. The basic instrumentation consisted of three miniature piezoelectric pressure transducers located 11.4, 29.2, and 47 centimeters from the end of the shock tube. These operated the start-stop circuits of two microsecond time-interval meters so that the velocity could be measured over two intervals for each run. A fourth pickup located 11.4 centimeters from the end of the tube was a calibrated SLM (Kistler Inst. Corp., type 601) pressure transducer. Its output, recorded on an oscilloscope, gave the pressure-time history in the reaction zone behind the reflected shock wave. The reflecting surface of the shock tube could be moved to within 0.63 centimeter of the SLM pressure transducer by inserting close fitting plugs into the tube.

In order to eliminate contamination of the helium driver gas by residual air, the driver section was evacuated to 1 torr or less and then purged with helium before filling.

The test section was always evacuated to about 4×10^{-3} torr and flushed with test gas before filling. This section was isolated from the pump by a cold trap cooled in liquid nitrogen and had a leak rate of 1 to 2×10^{-3} torr per minute.

The driven gases were nitrogen and various mixtures of argon, helium, and carbon dioxide. The mixtures were prepared by the method of partial pressures. The procedure was described in a previous paper (ref. 3).

RESULTS AND DISCUSSION

In each experiment the following data were obtained: initial temperature and pressures of driver and driven gas, incident shock velocities (over two intervals), and an oscilloscope record containing the pressure-time history. The shock velocities over the two intervals were generally found to be the same within the resolution of the measurement; therefore, attenuation was neglected. The pressure transducer was dynamically calibrated by plotting the measured p_5 against the calculated p_5 . Figure 2 is the calibration plot for the test gases used.

Pressure Histories

A survey of the literature showed that some of the typical pressure records reported were extremely difficult or impossible to interpret for the first 300 to 500 microseconds after passage of the reflected shock wave. This was due mainly to three things:

- (1) Acceleration response of the transducer
- (2) Excessive ringing of the transducer due to the mounting
- (3) Effect exerted on the pressure record by the interaction of the reflected shock wave and the boundary layer

This inability to determine the initial reflected shock pressure with any certainty lead us to question whether the flat-topped equilibrium state was not being confused with the tailored state. In order to illustrate the problem as it might arise from the third cause just listed, two reflected-pressure records were obtained in nitrogen at the same incident Mach number. Nitrogen was selected as the test gas because it is subject to strong bifurcation of the reflected shock near the wall, as described by Mark (ref. 4). Center (ref. 5) showed that the bifurcation becomes more pronounced as the shock recedes from the end wall. Thus, a pressure record obtained close to the end wall may clearly resolve p_5 , while one obtained farther away will have p_5 obscured by the effects of shock bifurcation.

The results of these tests are shown in figure 3. In figure 3(a), obtained at 0.63 centimeter from the end wall, the arrival of a strong disturbance from the contact surface at about 500 microseconds shows clearly that tailoring did not occur. But in the record of figure 3(b), which was obtained at 11.4 centimeters from the end wall, the interaction blends with the disturbance in the boundary layer that results from the more pronounced bifurcation. The record thus indicates a smoothly rounded pressure front followed by a plateau.

If the shock bifurcation were assumed to be responsible for all the curvature in a trace such as figure 3(b), then it would be quite possible to conclude that the flat portion signals the achievement of tailoring. In making this mistake, errors in pressure and temperature would arise amounting, in this particular case, to about 40 percent in the pressure and 180° K in the temperature. This is much too large an error for most experiments.

Thus, this experiment has shown that a greater degree of confidence can be achieved in tailoring by locating and mounting the pressure transducer so that the reflected shock pressure (p_5) can be measured and compared with theory. If this is impossible, then the equilibrium pressure should be measured and compared with the calculated p_5 since at the tailored conditions these two should be equal.

Tailoring

The first experiments were conducted with 7 percent CO_2 + 93 percent Ar driven by helium. Figure 1 shows a typical pressure-time history. The arrival of the reflected disturbance from the contact surface can be seen by the abrupt change in the pressure. The flat region after the interaction is the equilibrium state. The value of p_{e5} was determined by

using the ratio of the distances measured on the oscilloscope trace for $p_1 - p_5$ and $p_1 - p_e$ where p_1 was the initial pressure. This method has a small error since the initial pressure p_1 should be added to each measurement. However, this error is always less than 0.3 percent in p_{e5} , which is less than other sources of error in the determination. In figure 4 p_{e5} is shown plotted against the incident Mach number, which is also typical of the data for the other driver-driven gas combinations. Plotted also is the tailored Mach number calculated by equation (1) when ideal performance is assumed. This lack of agreement between experiment and theory is usual for most tailored experiments and is probably due to the nonideal behavior of most shock tubes.

A performance curve (P_{41} against M_s) for this gas combination is shown in figure 5. The ideal-performance curve is obtained for a real gas by using the relation

$$\left(\frac{P_{21}}{P_{41}}\right)^{\beta_4} = 1 - \frac{U_{21}A_{14}(\gamma_4 - 1)}{2} \quad (2)$$

which for a monatomic driver gas is

$$\left(\frac{P_{21}}{P_{41}}\right)^{0.2} = 1 - \frac{U_{21}A_{14}}{3} \quad (3)$$

where P_{21} and U_{21} are real gas shock properties. The experimental data is above the ideal curve, which is typical for most shock tubes. This behavior can be caused by a number of things such as diaphragm opening or shock attenuation. In any event, this higher than ideal P_{41} can effect the tailoring conditions because the temperature ratio T_{34} (eq. (1)) is calculated from the adiabatic expansion of the driver gas. And since the real p_4 is higher than ideal, the temperature T_3 will be lower than previously calculated. This would tend to lower the tailored Mach number calculated by means of equation (1), which is what was observed experimentally. Therefore, the tailoring calculations were performed by using the actual performance of the shock tube. The result of this calculation is shown in figure 4 and is clearly in close agreement with the experiment.

The Mach number at which tailoring occurs was calculated by using equation (1) and variable γ shock properties for the series of gas combinations studied. The results of these calculations are shown in table I along with the experimentally-observed tailored Mach number. For 7 percent CO_2 + 93 percent Ar and nitrogen tailoring calculations were also made for constant γ shock properties; these two examples showed

that the simpler constant γ calculation was as good as the variable γ calculation in the Mach number range of these experiments. It can be seen that all tailoring calculations fail when the ideal performance of the shock tube is used in the calculation. However, if the actual performance is used, the agreement with experiment is excellent.

The actual performance curves for all gas mixtures used were found to be about parallel to the ideal curves. This makes it possible to obtain the actual performance curve for a given driver-driven gas combination after just one test run. With the actual performance of the shock tube so obtained the tailored Mach number can be calculated, and the second experimental run should be extremely close to being tailored. If it should happen that the first P_{41} were somewhat in error, the second run should correct this and the third test should be tailored.

Contact Surface

Figure 6 is a pressure history for the tailored conditions predicted by the present method. The pressures p_5 and p_e are equal as required but the rise and fall of the pressure (hump) is out of character with the ideas of tailoring. This hump probably results from the mixing of the cold driver and hot driven gases in the contact zone. Evidence that the hump is associated with the contact surface can be provided by comparing experimental arrival times (time from passage of the reflected shock wave to return of the reflected disturbance from the contact surface) with calculated values.

Figure 7 shows a typical time-distance diagram of the kind used to calculate arrival times. Several of these were constructed, for various values of incident shock Mach number in the 7 percent CO_2 + 93 percent Ar mixture. Each diagram included both the trajectory followed by the contact surface in an ideal shock tube and the more realistic trajectory calculated by the analysis of Mirels (ref. 6) for a turbulent boundary layer. In the latter case, it was assumed that the gas mixture could be treated as pure argon for purposes of the calculation.

In order to calculate arrival times from these diagrams, the reflected disturbance from the contact surface was assumed to travel at the speed of sound in the undissociated and stationary gas behind the reflected shock wave. The results are plotted against M_g in figure 8. The contact surface trajectory calculated by the method of Mirels depends somewhat on initial pressure; two curves are therefore shown that correspond to the upper and lower extremes of initial pressure used in the present work.

The experimental arrival times were obtained by assuming that any abrupt change in the slope of the reflected shock pressure history indicated the arrival of the reflected disturbance from the contact surface. In tailored records, a small dip in pressure invariably occurred just before the hump and this was taken as the arrival of the disturbance (see fig. 6). At Mach numbers above the tailored value, the disturbance appeared as a sharp rise in the pressure, as in figure 1. In order to

extend the data below the tailored Mach number for helium driver gas, and to avoid reflected rarefaction waves whose arrival time is hard to read, some tests were made with an argon-helium driver. This driver mixture gave an easily read trace with a sharp pressure rise as in figure 1.

Figure 8 shows very good agreement between experimental arrival times and those expected on the basis of Mirels' contact surface trajectory. The arrival times calculated for an ideal contact surface were far outside the scatter of our data. The agreement between calculation and experiment suggests that a pressure hump is unavoidable even under tailored conditions, and as mentioned earlier, this interaction is probably due to the existence of a contact zone rather than a contact discontinuity. It is interesting to note that this zone evidently follows the trajectory predicted by Mirels, even though his analysis treats it as a discontinuity.

CONCLUDING REMARKS

Experiments showed that a flat-topped pressure record does not necessarily prove that tailoring had been achieved. This was because the equilibrium state, which also has a flat-topped pressure history, can be confused with the tailored state if the pressure transducer does not follow the initial reflected pressure history. However, with the criterion $p_e = p_5$ no such confusion can exist, since p_5 can be calculated and p_e measured.

An improved method for calculating the tailoring conditions has been presented. It requires the substitution of the actual shock tube performance (P_{41} against M_5) in the tailoring equations. Tailored pressure records can be achieved in two or three systematic experiments. Since no two shock tubes necessarily have the same performance curves, it follows from this work that the reflected conditions corresponding to tailored operation will be different in each tube, even though the driver-driven gas combination is the same.

Even at the tailored conditions a small hump was observed in the pressure record. This was shown to be associated with the contact surface. Measured arrival times (time from passage of the reflected shock wave to arrival of the reflected disturbance from the contact surface) in the Mach number range of 3.1 to 4.4 showed good agreement with those calculated by Mirels' analysis of the testing time between the shock wave and the contact surface.

REFERENCES

- (1) Hertzberg, A.; Smith, W. E.; Glick, H. S.; and Squire, W.: Modifications of the Shock Tube for the Generation of Hypersonic Flow. Rep. AD-789-A-2 (AEDC TN 55-15), Cornell Aeronautical Lab., Mar. 1955.
- (2) Glick, H. S.; Squire, W.; and Hertzberg, A.: A New Shock Tube Technique for the Study of High Temperature Gas Phase Reactions. Fifth Symposium (International) on Combustion, Fifth, Univ. of Pittsburgh, 1954, Reinhold Pub. Corp., 1955, pp. 393-402.

Brabbs and Belles

(3) Brabbs, Theodore A.; Belles, Frank E.; and Zlatarich, Steven A.: Shock-Tube Study of Carbon Dioxide Dissociation Rate. J. Chem. Phys., vol. 38, no. 8, Apr. 1963, pp. 1939-1944.

(4) Mark, Herman: The Interaction of a Reflected Shock Wave With the Boundary Layer in a Shock Tube. NACA TM 1418, 1958.

(5) Center, R. E.: The Interaction of a Reflected Shock Wave with the Laminar Boundary Layer in a Shock Tube. Aerodynamics Note 204, Aeronautical Res. Labs., Australian Defense Scientific Service, Dept. of Supply, Aug. 1962.

(6) Mirels, Harold: Shock Tube Test Time Limitation Due to Turbulent-Wall Boundary Layer. AIAA J., vol. 2, no. 1, Jan. 1964, pp. 84-93.

TABLE I. - CALCULATED AND OBSERVED INCIDENT MACH NUMBERS FOR TAILORING

Gas mixture, driven-driver	Incident shock Mach number, M_s					
	Experi- mental	Calculated				Variable γ
		Ideal performance		Actual performance		
		Constant γ	Variable γ	Constant γ	Variable γ	
0.07 CO ₂ + 0.93 Ar/He	3.60	3.81	3.80	3.61	3.62	
0.07 CO ₂ + 0.25 He + 68 Ar/He	3.15	-----	3.30	-----	3.16	
0.07 CO ₂ + 0.93 Ar/Ar + He	3.11	-----	3.17	-----	3.10	
0.03 CO ₂ + 0.97 Ar/He	3.62	-----	3.77	-----	3.62	
N ₂ /He	3.21	3.34	3.32	3.20	3.19	

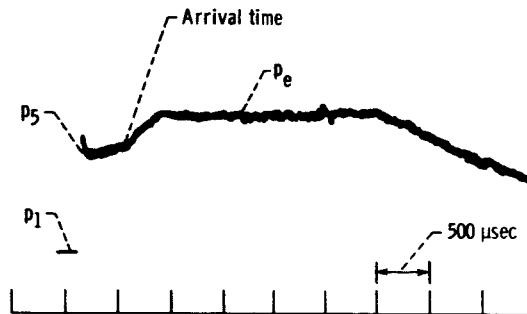


Figure 1. - Typical pressure history. Test gas, 3 percent CO_2 + 97 percent Ar; incident shock Mach number, 4.24.

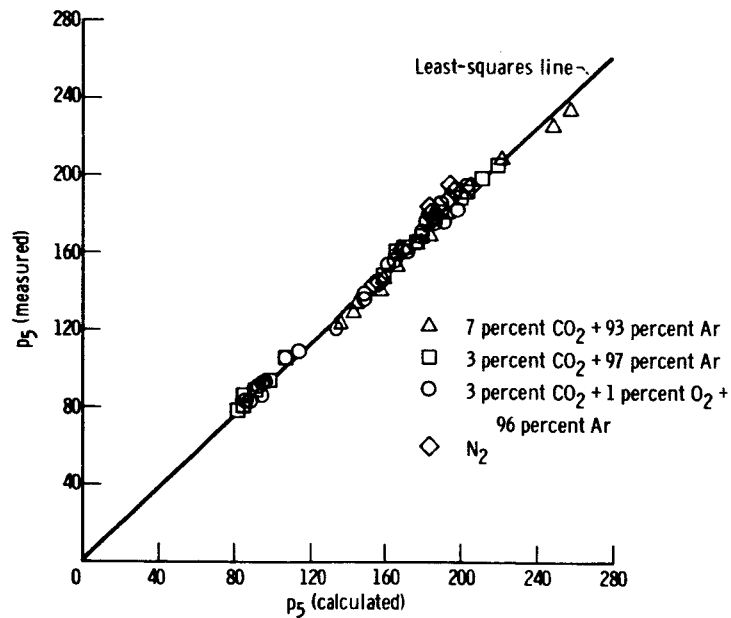
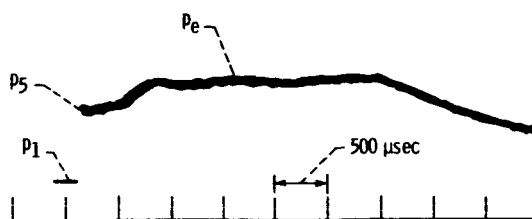
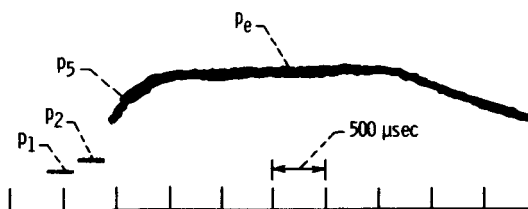


Figure 2. - Calibration curve for pressure transducer.



(a) Pressure pickup 0.64 centimeter from end wall.



(b) Pressure pickup 11.4 centimeters from end wall.

Figure 3. - Nitrogen pressure history at two locations in the shock tube. Incident shock Mach number, 3.87.

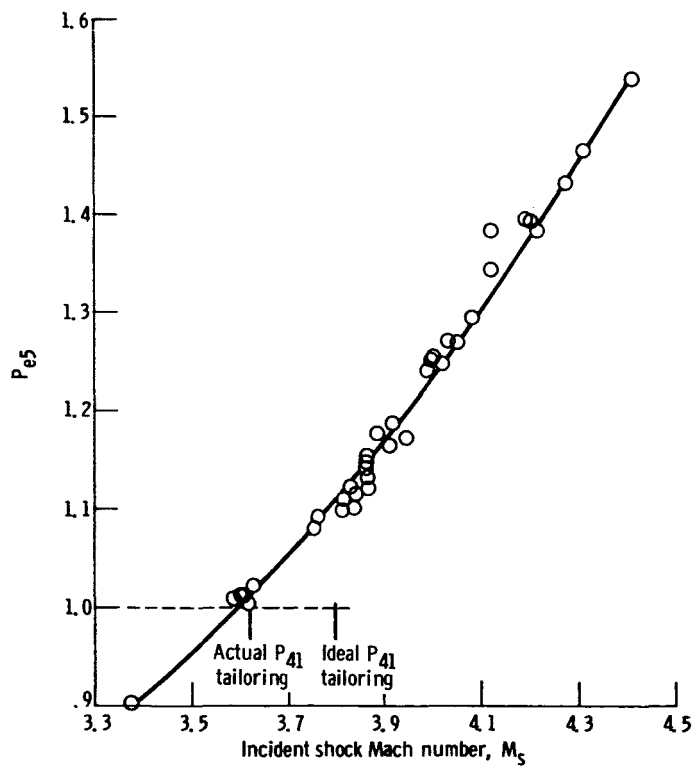


Figure 4. - Graph of P_{e5} against M_s for 7 percent CO_2 + 93 percent Ar driven by helium.

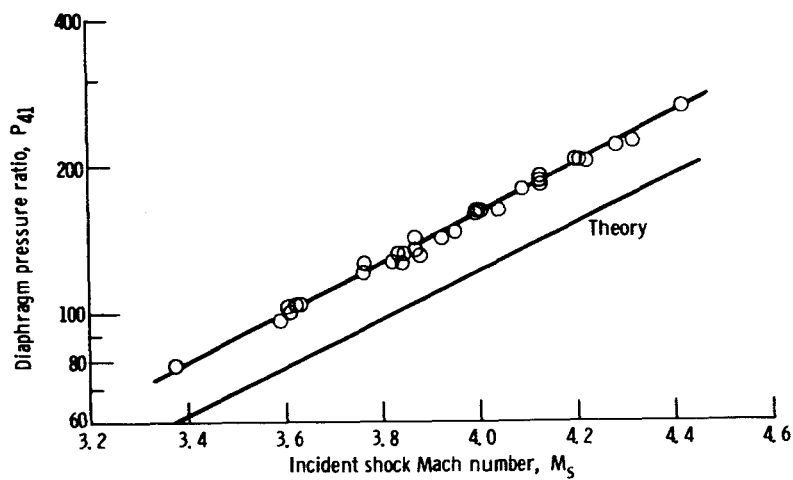


Figure 5. - Shock tube performance curve for 7 percent CO_2 + 93 percent Ar driven by helium.

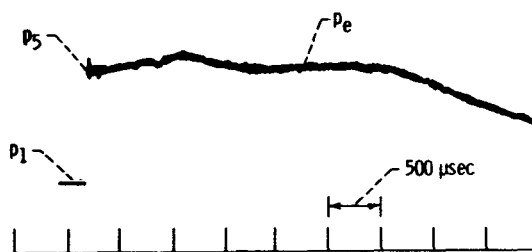


Figure 6. - Tailored pressure history for 7 percent CO_2 + 93 percent Ar driven by helium.

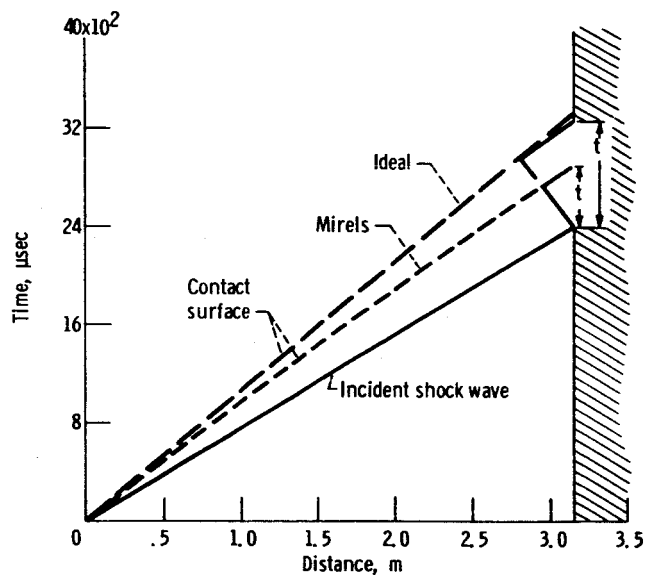


Figure 7. - Time-distance wave diagram.

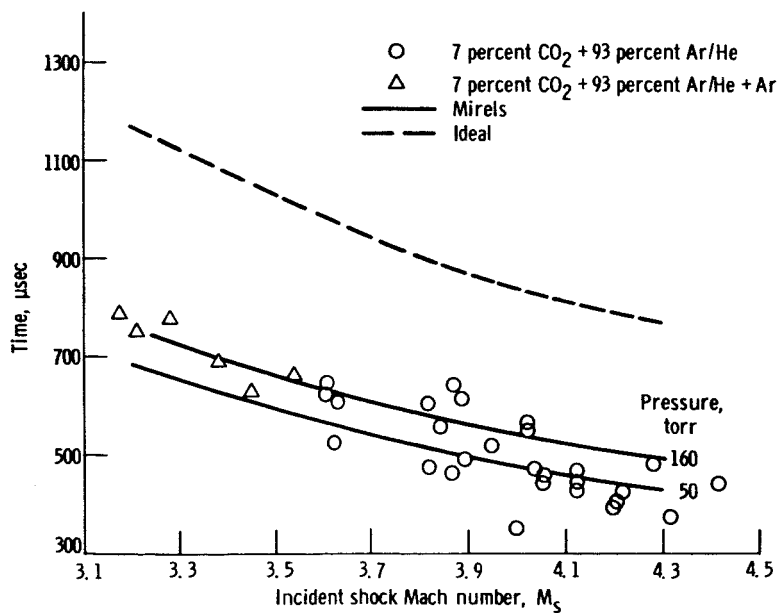


Figure 8. - Comparison of calculated and experimental arrival times.